Geophysical Research Letters®

Key Points:

- The development of surface precipitation in simulated trade-wind convection is decomposed into a formation and sedimentation phase
- As organization strengthens, less cloud condensate is converted into rain, but more rain reaches the ground as evaporation is suppressed
- Organization affects rain formation by modulating the local moisture environment, cloud vertical motion and microphysical properties

Correspondence to:

J. Radtke,
jule.radtke@uni-hamburg.de

Spatial Organisation Affects the Pathway to Precipitation in Simulated Trade-Wind Convection

Jule Radtke[1,2] , Raphaela Vogel[1] , Felix Ament[1] , and Ann Kristin Naumann[1,3]

[1]Center for Earth System Research and Sustainability, Meteorological Institute, Universität Hamburg, Hamburg, Germany, [2]International Max Planck Research School on Earth System Modelling, Hamburg, Germany, [3]Max Planck Institute for Meteorology, Hamburg, Germany

Abstract We investigate whether and how spatial organization affects the pathway to precipitation in large-domain hectometer simulations of the North Atlantic trades. We decompose the development of surface precipitation (P) in warm shallow trade cumulus into a formation phase, where cloud condensate is converted into rain, and a sedimentation phase, where rain falls toward the ground while some of it evaporates. With strengthened organization, rain forms in weaker updrafts from smaller cloud droplets so that cloud condensate is less efficiently converted into rain. At the same time, organization creates a locally moister environment and modulates the microphysical conversion processes that determine the raindrops' size. This reduces evaporation and more of the formed rain reaches the ground. Organization thus affects how the two phases contribute to P, but only weakly affects the total precipitation efficiency. We conclude that the pathway to precipitation differs with organization and suggest that organization buffers rain development.

Plain Language Summary Clouds in the trade-wind region organize into a variety of spatial patterns. We investigate how this spatial organization influences rain development in simulations of trade-wind convection. We divide the formation of surface precipitation into two phases. In the first phase, rain forms from the collision of cloud droplets or the collection of cloud droplets by raindrops. In the second phase, rain falls toward the ground while some of the rain evaporates. Our study shows that as organization strengthens, rain forms less efficiently, but a larger fraction of that rain reaches the ground as evaporation is reduced. Thus, organization in the simulations affects the way surface rain is generated. Our analyses suggest that it does so by modulating the cloud vertical motion in which rain forms, the local moisture environment through which rain falls and the microphysical conversion processes.

1. Introduction

What makes it rain? Precipitation was often neglected in studies of trade-wind convection because it was assumed that the convection is too shallow and short-lived to form precipitation (Siebesma, 1998; Stevens, 2005). Although there was already ample evidence of precipitation in the trade-wind region shown by Byers and Hall (1955) or Short and Nakamura (2000), it was not until attention to the trades and its clouds increased due to their large contribution to uncertainty in cloud feedbacks and climate sensitivity (Bony & Dufresne, 2005; Vial et al., 2013) that a more nuanced picture of trade-wind convection settled. The Rain In Cumulus over the Ocean (RICO) campaign (Rauber et al., 2007) was key in substantiating that precipitation is frequent in the trades (Nuijens et al., 2009), and highlighted that precipitation was often observed with arc-like cloud structures reminiscent of cold pool outflows (Snodgrass et al., 2009). Subsequent studies confirmed that trade-wind convection organizes into a variety of spatial structures—and that this often occurs in conjunction with precipitation development (Bony et al., 2020; Denby, 2020; Radtke et al., 2022; Schulz et al., 2021; Stevens et al., 2020; Vogel et al., 2021). How does spatial organization influence the development of (surface) precipitation in the trades? In this study, we exploit realistic large-domain hectometer (hm)-scale simulations of the North Atlantic trades (Schulz & Stevens, 2023) to investigate whether and how spatial organization affects the pathway to trade-cumulus precipitation.

Precipitation formation depends on dynamic, thermodynamic and microphysical interactions on different spatial and temporal scales. Due to the broad range of scales and processes involved, an understanding of rain formation and contributing processes remains challenging, even for warm, shallow trade cumulus. The representation of trade-cumulus precipitation among large-eddy simulations (LES) differs largely (van Zanten et al., 2011). An understanding of how spatial organization relates to warm rain development could help interpret and reduce these

differences. Organization may affect how efficiently rain forms and how much evaporates through modulating mesoscale circulations or the local moisture environment (Narenpitak et al., 2021; Seifert & Heus, 2013). Moreover, understanding the relationship between spatial organization and precipitation may also be key to disentangle the mechanisms of organization and explain its influence on the total cloud cover in the trades, a prerequisite to further constrain the climate feedback of the trades (Bony et al., 2020; Nuijens & Siebesma, 2019).

Analyzing rain radar measurements upstream of Barbados taken during the EUREC⁴A field campaign (Hagen et al., 2021; Stevens et al., 2021), Radtke et al. (2022) show that while the occurrence of trade-wind precipitation is related to organized cells, the mean rain rate varies largely independently of the cells' *degree* of organization. However, scenes with similar precipitation but different degrees of spatial organization also differed in the moisture environment. Similarly, Yamaguchi et al. (2019) find that in idealized LES, shallow cumulus precipitation varies little, but the sizes and spatial distribution of clouds differ in response to large changes in the aerosol environment. Could spatial organization be a mechanism to maintain precipitation in different environments, enabling or creating a different pathway to precipitation?

To answer this question on a process-level, we make use of large-domain hm-scale simulations of the North Atlantic trades that were run for the period January–February 2020 during the EUREC⁴A campaign (Bony et al., 2017; Schulz & Stevens, 2023; Stevens et al., 2021) and were designed to explore spatial organization on the mesoscale (20–200 km). We follow the method of Langhans et al. (2015) and Lutsko and Cronin (2018) and decompose the development of surface precipitation into two phases, (a) a formation phase, in which cloud condensate is converted into rain water, and (b) a sedimentation phase, in which the formed rain water falls toward the ground while part of it evaporates. Section 2 describes the setup and microphysical scheme of the simulations and our analysis method. Section 3.1 shows that spatial organization in scenes of $\mathcal{O}(100 \text{ km})$ influences how these two phases contribute to the development of trade-wind precipitation. Section 3.2 explains such behavior and interprets it as a form of buffering, before we conclude in Section 4.

2. Methods

2.1. EUREC⁴A Large-Domain ICON Hm-Scale Simulations

The simulations are conducted with the LES configuration of the ICOsahedral Non-hydrostatic (ICON) model (Dipankar et al., 2015). ICON solves the compressible Navier–Stokes equations on an unstructured grid as detailed in Zängl et al. (2015) and Dipankar et al. (2015). To explore mesoscale convective variability, the simulations are performed with a relatively fine hectometer-scale mesh over a large domain of $\mathcal{O}(1,000 \text{ km})$ for an extended EUREC⁴A campaign period from 9 January to 19 February 2022. They are realistically forced with initial and boundary data from a storm resolving simulation at 1.25-km grid spacing, which is in turn initialized and nudged at its lateral boundaries to the atmospheric analysis of the European Centre for Medium-Range Weather Forecasts (similar to Klocke et al., 2017). Here, we analyze a simulation with 625 m grid spacing that covers the western tropical Atlantic from 60.25 to 45.0°W and 7.5–17.0°N, spanning about 1,650 km in the east-west direction, and 1,050 km in the north-south direction. In the vertical, 150 levels are used, resulting in 70 and 85 m vertical resolution at 1,000 and 2,000 m height, respectively.

Schulz and Stevens (2023) show that this simulation reproduces differences in the mesoscale structure underlying the canonical forms of trade cumulus organization of Stevens et al. (2020), as well as variability in precipitation, which makes them a good starting point to investigate how the process of precipitation may vary with spatial organization. A nested 312 m simulation does not show a substantially greater skill in representing different cloud organizations or rain rates (Schulz & Stevens, 2023) and shows the same qualitative behavior in our analysis (not shown). We refer the reader to Schulz and Stevens (2023) for an in-depth observational evaluation and comparison of the simulations. In Supporting Information S1 we summarize and discuss the evaluation of the simulation properties relevant for our work.

In the simulations, turbulence is parameterized with the Smagorinsky scheme, microphysics with the two-moment mixed-phase bulk microphysics scheme of Seifert and Beheng (2006) and a cloud condensation nuclei concentration of 130 cm⁻³ is prescribed. Warm rain is produced by autoconversion and accretion, defined following Seifert and Beheng (2001) as $\frac{\partial L_r}{\partial t}|_{au} \sim L_c^2 \bar{x}_c^2$ and $\frac{\partial L_r}{\partial t}|_{acc} \sim L_c L_r$, where L_r is rain water content, L_c cloud water content and $\bar{x}_c = \frac{L_c}{N_c}$ mean mass of cloud droplets with cloud droplet number concentration N_c. To quantify the production
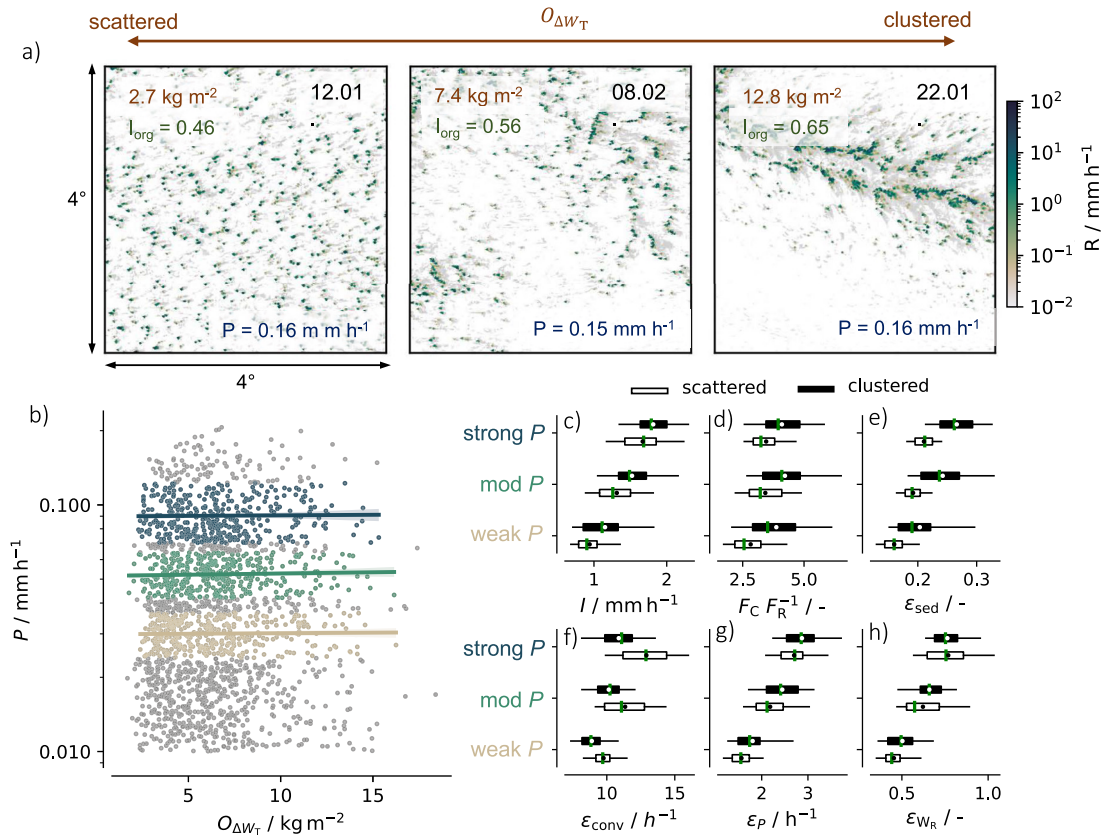
Figure 1. (a) Three example scenes with similar scene-averaged precipitation P (i.e., rain amount, blue) but different degrees of organization characterized by $O_{\Delta W_T}$ (orange) and the I_{ORG} (green). Color shading denotes rain rate R. Gray shading denotes cloud albedo calculated from simulated cloud liquid water path. (b) P as a function of $O_{\Delta W_T}$. Three different rain regimes with weak $P = (0.024, 0.037)$, mod $P = (0.042, 0.064)$ and high $P = (0.07, 0.12)$ are distinguished. (c) Rain intensity I, (d) cold pool fraction F_C per rain fraction F_R, (e) sedimentation efficiency ϵ_{sed}, (f) conversion efficiency ϵ_{conv}, (g) precipitation efficiency ϵ_P, and (h) rain water loading efficiency $\epsilon_{W_R} = \frac{W_R}{W_L}$, with W_R as rain water path, shown for the three precipitation regimes, separated into a clustered ($O_{\Delta W_T} > 70$th percentile, filled bars) and scattered sample ($O_{\Delta W_T} < 30$th percentile, empty bars). The green line denotes the median, the dot the mean, the box the interquartile range and the whiskers denote the 5th and 95th percentile.

of rain, we recalculate the autoconversion and accretion rates from the instantaneous 3D model output of cloud water, rain water and cloud effective radius r_{eff}, from which the volume radius r_v is derived by $(r_v/r_{eff})^3 = 0.8$ (Freud & Rosenfeld, 2012) to calculate the cloud droplets' mean mass. The 3D output is available every 3 hr.

2.2. Investigating Spatial Organisation and the Pathway to Precipitation

We investigate spatial organization in scenes of $4 \times 4°$ (about 450×450 km), an area extent similar to previous studies (George et al., 2023; Radtke et al., 2022). Figure 1a shows three scenes with different degrees of organization as an example. To mask high ice clouds, scenes with outgoing longwave radiation <275 W m^{-2} are excluded (changes in the threshold do not affect our qualitative results), as well as scenes with little precipitation $P < 0.01$ mm hr^{-1}. Here and if not indicated otherwise, we refer to domain mean values. In total about 2,000 scenes are used in the analyses (about 7 scenes across the domain every 3 hr).

Following Bretherton and Blossey (2017) and Narenpitak et al. (2021), we assess the degree of spatial organization as mesoscale variability in the moisture field, which is closely connected to the cloud structure. First, the total water path, W_T, defined as the sum of vertically integrated water vapor, cloud condensate, and rain, is coarse-grained into tile sizes of 20×20 km^2, representing variability associated with the mesoscale (Orlanski, 1975). Subsequently, the coarse-grained W_T is binned into quartiles and the difference between the fourth and first quartile is calculated as organization metric $O_{\Delta W_T}$. This metric classifies the three example scenes from weakly organized (low $O_{\Delta W_T}$) on the left, to more strongly organized (high $O_{\Delta W_T}$) on the right. This is

consistent with a visual subjective classification of the cloud field, the nearest neighbor clustering technique I_{ORG} (Tompkins & Semie, 2017), and the cloud pattern classification of Stevens et al. (2020). According to this classification, the left scene depicts a Gravel pattern, characterized by scattered convection (low I_{ORG}), and the right scene a Fish pattern, characterized by more clustered convection (higher I_{ORG}). An overview and more in-depth discussion of different organization metrics has recently been given by, for example, Janssens et al. (2021).

To investigate the pathway to trade-wind precipitation, we decompose the development of surface rain following Langhans et al. (2015) and Lutsko and Cronin (2018) into (a) a formation phase and (b) a sedimentation phase. In phase (a), warm rain initially forms by the merging of small cloud droplets, parameterized by the autoconversion rate. Additionally, rain is produced as falling raindrops collect cloud droplets, parameterized by the accretion rate. Autoconversion dominates the formation of rain especially for young or short-lived clouds, while accretion contributes more to the formation of rain as clouds live longer and there is more time available for the collision-coalesence process to take place (Feingold et al., 2013). To quantify how efficient the formation of rain water is, we define a conversion efficiency

$$\epsilon_{\text{conv}} = \frac{C_{\text{R}}}{W_{\text{L}}},\tag{1}$$

where $C_{\text{R}} = C_{\text{Auto}} + C_{\text{Acc}}$ with C_{Auto} and C_{Acc} denoting the vertically integrated autoconversion and accretion rates and W_{L} the cloud liquid water path. In phase (ii), the rain formed by autoconversion and accretion sediments toward the ground. During this process, some rain evaporates. The rain that does not evaporate reaches the ground as surface precipitation, P, so that we call

$$\epsilon_{\text{sed}} = \frac{P}{C_{\text{R}}} = 1 - \epsilon_{\text{evap}}\tag{2}$$

the sedimentation efficiency with ϵ_{evap} the evaporation efficiency. Please note that we do not refer to in-cloud sedimentation here, but, following Langhans et al. (2015) and Lutsko and Cronin (2018), we use sedimentation efficiency to refer to how much rain reaches the ground instead of evaporating.

The product of the conversion and sedimentation efficiencies describes how much cloud water in a given time interval is returned to the surface as precipitation, representing an overall precipitation efficiency ϵ_{P}, for example, as used in Lau and Wu (2003):

$$\underbrace{\frac{P}{W_{\text{L}}}}_{\epsilon_{\text{P}}} = \underbrace{\frac{C_{\text{R}}}{W_{\text{L}}}}_{\epsilon_{\text{conv}}} \cdot \underbrace{\frac{P}{C_{\text{R}}}}_{\epsilon_{\text{sed}}} .\tag{3}$$

Said differently, the inverse of ϵ_{P} is the time it takes to remove all cloud water at the given precipitation rate, thus describing a typical residence time. It is to note that precipitation efficiency itself has no unique definition (e.g., Sui et al., 2020). Different results may emerge for different definitions and also depend on local versus domain-mean views. However, using an approximation of the condensation rate following Muller and Takayabu (2020) instead of liquid water path in Equation 3 results in the same qualitative behavior. Here, we mainly exploit precipitation efficiency and its decomposition into conversion and sedimentation efficiencies as a proxy for the pathway that precipitation development takes.

3. Results

3.1. The Pathway to Precipitation Varies With Organisation

The hm-scale simulations reproduce EUREC⁴A observations in that scene precipitation in the trades varies mainly independently of organization (Radtke et al., 2022). This is depicted in the example scenes in Figure 1a, which display a similar rain rate but vastly different degrees of organization, and is more quantitatively shown in Figure 1b. In the simulations, scene rain rates vary up to 0.2 mm hr^{-1} as shown in Figure 1b, which compares well to rain rates observed in the RICO (Nuijens et al., 2009) and EUREC⁴A campaign (Radtke et al., 2022). In the following, we will show whether also the pathway to these rain rates is similar or in how far organization affects how these rain rates are generated, and could thus be a process to maintain precipitation in different environments.

To investigate this, we group our sample of scenes into three precipitation regimes, a weak, a moderate, and a strong precipitation regime, as visualized in Figure 1b. In each regime, we define more organized scenes as
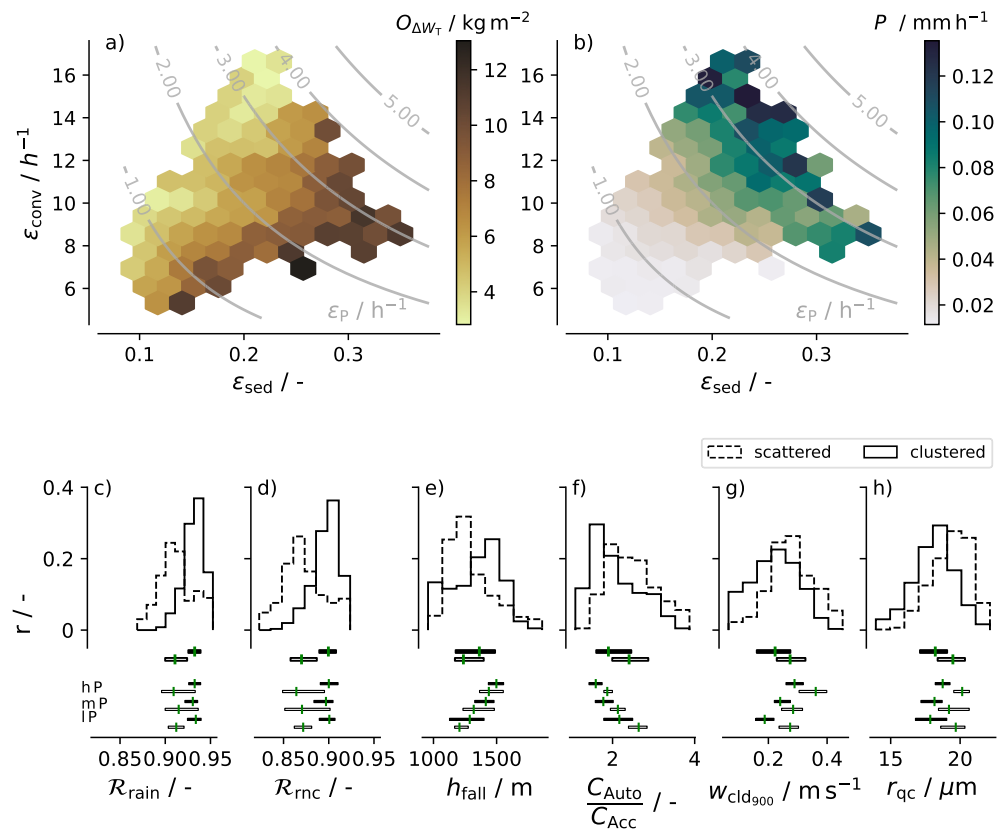
Figure 2. (a) Degree of mesoscale organization $O_{\Delta W_T}$ and (b) precipitation P (shading) as a function of conversion efficiency ϵ_{conv} and sedimentation efficiency ϵ_{sed}. Contour lines denote precipitation efficiency from Equation 3. Relative frequency of (c) rain-conditioned relative humidity $\mathcal{R}_{rain}$, (d) rain-and-no-cloud-conditioned relative humidity $\mathcal{R}_{rnc}$, (e) fall height h_{fall}, (f) ratio of autoconversion C_{Auto} to accretion C_{Acc}, (g) cloud-conditioned vertical velocity at 900 hPa $w_{cld_{900}}$ and (h) mean cloud droplet radius r_{qc} for the scenes separated into scattered (dashed line, empty bars) and clustered (solid line, filled bars) convection and divided into three precipitation regimes (as in Figure 1, hP denoting the high P regime, mP the mod P regime and lP the low P regime). Horizontal boxes denote the interquartile range, vertical lines the median.

$O_{\Delta W_T} > $ 70th percentile and less organized scenes as $O_{\Delta W_T} < $ 30th percentile, which we refer to as clustered and scattered sample, respectively. The conclusions are insensitive to the exact choice of threshold. This relative way of differentiating between more and less organized scenes is based on the simulated distribution of organization, which will vary depending on how variable the large-scale conditions are and possibly which specific model is used.

Figure 1c shows that, instead of the mean rain rate, organization tends to increase the rain intensity, which is again in line with observational studies of trade-wind (Radtke et al., 2022) and deep convection (Louf et al., 2019). That is, clustered convection produces the same amount of scene precipitation as scattered convection with more intense rain covering a smaller area. Detecting cold pools based on the calculation and criterion of a mixed layer height smaller than 400 m following Touzé-Peiffer et al. (2022), clustered scenes are also populated by more cold pools as shown in Figure 1d, possibly associated with this increase in rain intensity. In clustered scenes, the cold-pool fraction is about four times greater than the rain fraction, whereas in scattered scenes it is about three times greater. These findings may already hint to an altered precipitation process in more organized compared to less organized scenes.

We investigate the relationship between organization and the conversion, sedimentation and total precipitation efficiency (Equation 3), shown in Figure 2a. Organization maximizes toward the lower right of the phase space, at low conversion and high sedimentation efficiencies. An increase in the degree of organization is thus related to a decrease in how efficiently cloud water is converted into rain and an increase in how efficiently rain sediments as a greater fraction of rain reaches the ground instead of evaporating. The sedimentation efficiency varies between

0.1 and 0.3, emphasizing that much of the rain evaporates, as reported by Naumann and Seifert (2016) or Sarkar et al. (2022). Figure 2b shows that precipitation maximizes toward the upper right of the same phase space, that is, at high sedimentation and conversion efficiencies. Within a precipitation regime, as shown in Figures 1e and 1f, rain thus sediments more efficiently but forms less efficiently in clustered compared to scattered scenes. This behavior is slightly enhanced in regimes with stronger precipitation.

The product of the conversion and sedimentation efficiencies gives the overall precipitation efficiency, denoted in the contour lines in Figure 2. Precipitation efficiency varies closely with precipitation and lies mostly between 1 hr^{-1} and 3 hr^{-1}. That one to three times the cloud liquid water path precipitates per hour emphasizes the rapid turnover and rain formation in trade-wind clouds, which with tops greater than 2,500 m "usually rain within half an hour" (Squires, 1958). Because conversion efficiency decreases but sedimentation efficiency increases with organization, contours of precipitation efficiency and organization lie perpendicular to each other in Figure 2a. This means that organization and precipitation efficiency, like precipitation, vary mainly independently of each other. Composited on the three different precipitation regimes, Figure 1g shows that precipitation efficiency compared to the conversion and sedimentation efficiency varies only weakly with organization with a slight tendency to increase with organization. Analyzing the ratio of rain water path to cloud water path instead of the ratio between precipitation and cloud liquid water path gives the same result (Figure 1h).

Our analysis thus suggests that organization weakly affects precipitation efficiency in terms of how much cloud water precipitates on average, but changes the pathway to precipitation in terms of how the formation versus sedimentation phases contribute to the development of surface precipitation. Next, we investigate physical mechanisms behind this behavior.

3.2. How Does Organisation Affect the Pathway to Precipitation?

3.2.1. Sedimentation Efficiency

The sedimentation efficiency describes how much rain reaches the ground instead of evaporating. Following Lutsko and Cronin (2018), we suggest that ϵ_{sed} should scale to a first approximation with the moisture environment through which the rain falls, or more explicitly with the saturation deficit, and the time it takes the rain to fall:

$$\epsilon_{evap} = 1 - \epsilon_{sed} \sim (1 - \mathcal{R}_{rain}) \cdot t_{fall} = (1 - \mathcal{R}_{rain}) \cdot \frac{h_{fall}}{v_{fall}}, \qquad (4)$$

where $\mathcal{R}_{rain}$ is the averaged relative humidity the falling rain experiences, that is, conditioned on pixels with rain water $q_r > 0.001$ g kg^{-1} (van Zanten et al., 2011), and t_{fall} the average fall time, which depends on the average fall height h_{fall} and fall velocity v_{fall}. The higher the saturation deficit or the longer the rain falls and thus has time to evaporate, the higher evaporation and the lower the amount of rain reaching the ground.

We hypothesize that organization influences the moisture environment through which rain falls, since it manifests itself in an uneven (horizontal) distribution of moisture, as also used in our metric of organization. Figure 2c shows that in the simulations, rain in clustered scenes indeed typically falls through a more humid environment with a lower saturation deficit than in scattered scenes. This is true for all precipitation regimes, with little variations in $\mathcal{R}_{rain}$ between precipitation regimes. We find that rain falls through a moister environment because the environment outside of or beneath clouds is closer to saturation (about 3%, Figure 2d), not just because more rain may fall within than outside of clouds, for example, due to different wind shears and cloud tilts. This is in line with the idea that clouds in more organized scenes develop preferentially in the parts of the domain with moister, more favorable thermodynamic conditions, for example, preconditioned by former clouds (sometimes called mutual-protection hypothesis, Seifert & Heus, 2013) or established through enhanced moisture transport into anomalously moist patches by mesoscale circulations (George et al., 2023; Narenpitak et al., 2021). That way, clusters may form, clouds may be better protected from updraft buoyancy reduction through entrainment (Becker et al., 2018; Mapes & Neale, 2011), and less rain evaporates.

Besides the moisture environment, organization could also influence the fall time of the rain drops by modulating the fall height or fall velocity (Equation 4). We define the fall height h_{fall} as average height where rain is produced by autoconversion and accretion. Analyzing h_{fall} shows that rain in clustered convection falls on average from slightly higher heights than in scattered convection (Figure 2e), related to a tendency of clouds to grow deeper
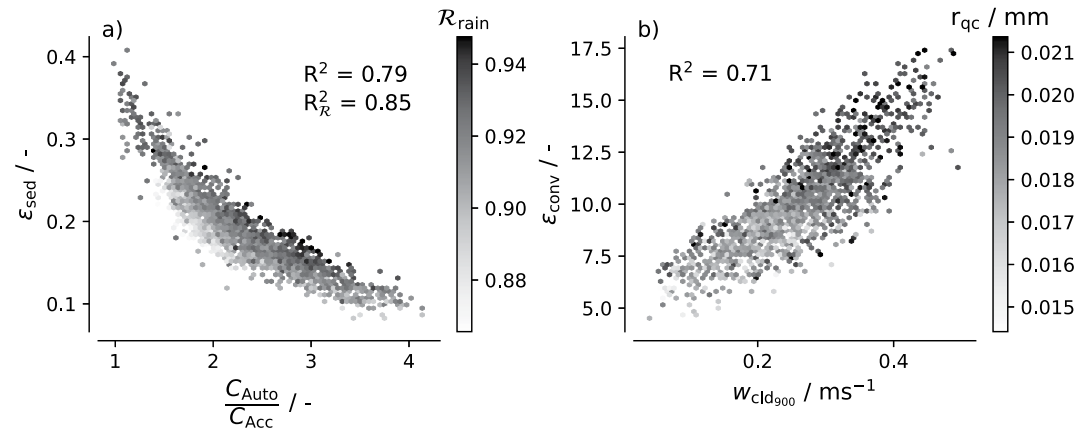
Figure 3. (a) Sedimentation efficiency ϵ_{sed} as a function of the relative importance of autoconversion C_{Auto} and accretion C_{Acc}. Shading denotes the rain-conditioned relative humidity $\mathcal{R}_{rain}$ (b) Conversion efficiency ϵ_{conv} as a function of cloud-conditioned vertical velocity at 900 hPa $w_{cld_{900}}$. Shading denotes the mean cloud droplet radius r_{qc}.

and inversion heights to increase with organization (not shown). If the fall velocity stays unchanged, this would suggest that organization slightly increases the time it takes for rain to fall to the ground, which would act to enhance, not to reduce evaporation in more strongly organized scenes.

For the mean fall velocity, multiple factors, for example, the strength of up- and downdrafts and the raindrops' size are decisive. The raindrop size was not included in the model output but the way rain is produced, that is, in how far autoconversion versus accretion dominates the formation of rain, may serve as a proxy for the raindrops' size. Figure 3a shows that in how far autoconversion versus accretion contributes to rain formation explains 79% of the variations in sedimentation efficiency. Because autoconversion produces initial "embryo" raindrops when cloud droplets merge, whereas accretion is responsible for the growth of raindrops through further collection of cloud droplets, an increased contribution of accretion to rain formation indicates that raindrops have grown larger. Figure 2f shows that in more organized scenes the contribution of accretion to rain formation is increased. Raindrops in more organized scenes are thus likely larger. Larger rain drops fall faster, reducing the fall time and hence evaporation.

When including, in addition to the relative importance of autoconversion and accretion, $\mathcal{R}_{rain}$ as additional predictor, 85% of the variations in sedimentation efficiency can be explained. Additionally including h_{fall} does not explain further variations. Our analysis thus suggests, as illustrated in Figure 4, that organization reduces evaporation and increases the sedimentation efficiency because rain in more organized scenes is increasingly produced by accretion so that raindrops are larger and fall faster, through an environment that is moister.
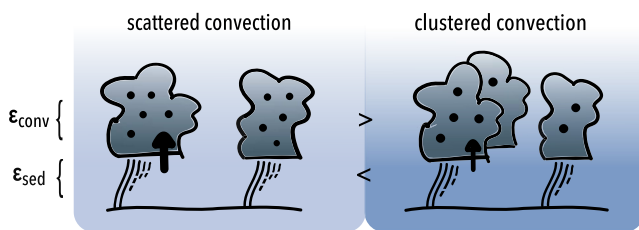
3.2.2. Rain Formation Efficiency

Rain starts to form when sufficient cloud water has been produced and cloud droplets have grown to raindrop size (e.g., Seifert & Stevens, 2010). To initiate and grow cloud particles the air's saturation is important and influenced by thermodynamic conditions as well as vertical motions (Rogers & Yau, 1996).

In the simulations, organization influences the clouds' vertical motion. Figure 2g shows that in clustered scenes the mean in-cloud vertical motion near cloud base, $w_{cld_{900}}$ (cloud-conditioned, i.e., where cloud water $q_c > 0.01$ g kg^{-1}, and at 900 hPa), is weaker than in more scattered scenes. This initially appears surprising. It can be attributed, in part, to the presence of stronger downdrafts, for example, the 25th percentile of $w_{cld_{900}}$ is lower, and in part to weaker updrafts as the mean and median cloud upward motion is reduced (not shown). Bao and Windmiller (2021) found a similar decrease in vertical motions with organization in deep convection. Because

Figure 4. Conceptual illustration of the simulated pathway to surface precipitation in weakly (left) versus strongly (right) organized convection: For similar surface precipitation, as organization strengthens, rain forms in a locally moister environment (shading) in weaker updrafts (arrow) and increasingly from accretion indicating larger raindrops (dots). As a consequence, evaporation is reduced, so that more rain reaches the ground compared to scattered convection (ϵ_{sed} is larger), but rain forms less efficiently (ϵ_{conv} is smaller), with both changes having a compensating, that is, buffering effect on surface rain development.

organization creates more favorable thermodynamic conditions for cloud and rain formation with a local increase in humidity (Figures 2c and 2d), this may allow clouds and rain to develop in less favorable dynamic conditions, that is, at weaker mean upward motions. Additionally, the cloud population in more organized scenes could also consist of more long-lived, older clouds as indicated by the increased contribution of accretion to rain formation. In these, updrafts may have already started to weaken. Future analysis of the cloud lifecycle with respect to organization may therefore potentially reconcile the apparent contradiction between the expected larger raindrops resulting from increased accretion and the presence of weaker updrafts.

More organized scenes also differ from less organized scenes in the mean cloud droplet radius. Figure 2h shows that in clustered scenes, the mean cloud droplet radius is smaller by about 1.3 μm than in scattered scenes. From moderate to high precipitation, this difference increases, which is in line with the strong decrease in conversion efficiency at high precipitation. The smaller cloud droplet size in more organized scenes agrees with the weaker vertical motions. Besides, Cooper et al. (2013) showed that mixing and entrainment affect cloud droplet growth and the onset of precipitation. By changing the mixing characteristics of clouds, organization might also influence the cloud droplets' size.

Figure 3b shows that 70% of the variations in conversion efficiency are explained by the mean vertical motion at cloud base, to which the mean cloud droplet size is correlated. To conclude and as illustrated in Figure 4, our analyses suggest that organization reduces the efficiency with which cloud water is converted into rain water because rain in clustered scenes forms in weaker updrafts that correlate with smaller mean cloud droplets. We hypothesize that this is because favorable thermodynamic conditions may compensate for weaker dynamic conditions and organization may affect the lifetime as well as the mixing characteristics of the cloud population.

3.2.3. Buffering

Organization is associated with an increase in the sedimentation efficiency, but a decrease in the formation efficiency and thus influences rain development in an opposing or stabilizing way. This may be interpreted as a form of buffering. Buffering as introduced in Stevens and Feingold (2009) denotes that if there are different pathways to reach the same final state, these buffer or stabilize the system against disruptions to any particular pathway. For example, cloud deepening as a dynamical response to increased droplet number concentration has been shown to buffer the microphysical suppression of precipitation (Seifert et al., 2015). Our analyses suggest that organization can have a stabilizing, that is, buffering, relationship to rain development, due to opposing effects on rain formation and sedimentation efficiency, as illustrated in Figure 4. While in more scattered convection, rain development is characterized by efficient conversion of cloud water into rain water but also subsequent evaporation is strong, in more clustered convection, increased sedimentation efficiency compensates for a decreased conversion efficiency. These variations on the pathway to precipitation by organization may be an additional explanation for why rain development is so common in the trades. They also offer an explanation for the observed (Radtke et al., 2022) and simulated large independence between rain amount and organization rather than a reinforcement.

Based on our results, we hypothesize that such buffering effect of organization on rain development is related to (a) an interplay of thermodynamic and dynamic conditions and (b) (life)time effects. Regarding (a), more favorable thermodynamic conditions may allow clouds to develop under less favorable dynamic conditions. Regarding (b), the increased contribution of accretion to rain formation with organization indicates longer-lived, older clouds, in agreement with the expectation of more sustained convection with organization. In older, more mature clouds, the rain formation process had time to evolve (Feingold et al., 2013), so that raindrops may grow larger and fall out more efficiently, while updrafts may have already weakened so that further rain forms less efficiently.

4. Summary and Conclusions

We exploit realistic large-domain hm-scale simulations of the North Atlantic trades to investigate whether and how organization affects the pathway to trade-cumulus precipitation. We decompose the development of surface precipitation following Langhans et al. (2015) into a formation phase, where cloud condensate is converted to rain, and a sedimentation phase, where the formed rain falls to the ground while some of it evaporates. In the simulations, organization affects how these two phases contribute to rain development, summarized schematically in Figure 4.

With strengthened organization, rain in the hm-scale simulations forms in and falls through a locally more humid environment. Additionally, rain is increasingly produced by accretion rather than autoconversion, which indicates

that clouds live longer and raindrops grow larger. Larger raindrops, that fall through a more humid environment experience less evaporation, leading to an increase in the sedimentation efficiency. The relative importance of accretion and autoconversion explains 79% of the variations in sedimentation efficiency, increasing to 85% when including the rain-conditioned relative humidity as an additional predictor. A locally more humid environment is in line with the idea that an increase in organization is related to more humid patches in which clouds develop and which protect clouds from dilution and raindrops from evaporation. It may suggest that organization also increases the efficiency with which cloud condensate is converted to rain. However, in more organized scenes rain forms in weaker updrafts (as in Bao and Windmiller, 2021), and from smaller cloud droplets. This leads to cloud water being less efficiently converted to rain, in agreement with radiative-convective equilibrium simulations by Lutsko and Cronin (2018). 71% of the variations in conversion efficiency are explained by the in-cloud vertical motion at cloud base, to which the cloud droplet size is correlated. Possibly because the thermodynamic environment is more favorable with organization, less favorable dynamic conditions already allow for rain formation, or lifetime effects may play a role here. Both effects, the increase in sedimentation efficiency and the decrease in conversion efficiency, largely compensate, so that organization does not substantially affect the total precipitation efficiency.

Our analyses suggest that organization can buffer rain development via opposing effects on the rain formation and sedimentation efficiencies. They offer an explanation for the observed and simulated large independence between rain amount and organization. While in less organized scenes rain development is characterized by efficient conversion of cloud condensate into rain, in more organized scenes more efficient sedimentation, as evaporation is suppressed, increasingly contributes to surface rain development. It remains to be shown in how far these results carry over to other models and observations. In our simulations, we conclude that the pathway to precipitation differs with spatial organization.

Conflict of Interest

The authors declare no conflicts of interest relevant to this study.

Data Availability Statement

The simulation output is freely available and can be easily accessed via the EUREC^{4}A-Intake catalog at https://github.com/eurec4a/eurec4a-intake as described at https://howto.eurec4a.eu/simulations. Detailed information about the simulations is given in Schulz and Stevens (2023).

References

Bao, J., & Windmiller, J. M. (2021). Impact of microphysics on tropical precipitation extremes in a global storm-resolving model. *Geophysical Research Letters*, *48*(13), e2021GL094206. https://doi.org/10.1029/2021GL094206

Becker, T., Bretherton, C. S., Hohenegger, C., & Stevens, B. (2018). Estimating bulk entrainment with unaggregated and aggregated convection. *Geophysical Research Letters*, *45*(1), 455–462. https://doi.org/10.1002/2017GL076640

Bony, S., & Dufresne, J.-L. (2005). Marine boundary layer clouds at the heart of tropical cloud feedback uncertainties in climate models. *Geophysical Research Letters*, *32*(20), L20806. https://doi.org/10.1029/2005GL023851

Bony, S., Schulz, H., Vial, J., & Stevens, B. (2020). Sugar, gravel, fish, and flowers: Dependence of mesoscale patterns of trade-wind clouds on environmental conditions. *Geophysical Research Letters*, *47*(7), e2019GL085988. https://doi.org/10.1029/2019GL085988

Bony, S., Stevens, B., Ament, F., Bigorre, S., Chazette, P., Crewell, S., et al. (2017). EUREC4A: A field campaign to elucidate the couplings between clouds, convection and circulation. *Surveys in Geophysics*, *38*(6), 1529–1568. https://doi.org/10.1007/s10712-017-9428-0

Bretherton, C. S., & Blossey, P. N. (2017). Understanding mesoscale aggregation of shallow cumulus convection using large-eddy simulation. *Journal of Advances in Modeling Earth Systems*, *9*(8), 2798–2821. https://doi.org/10.1002/2017MS000981

Byers, H. R., & Hall, R. K. (1955). A census of cumulus-cloud height versus precipitation in the vicinity of Puerto Rico during the winter and spring of 1953-1954. *Journal of the Atmospheric Sciences*, *12*(2), 176–178. https://doi.org/10.1175/1520-0469(1955)012⟨0176:ACOCCH⟩2.0.CO;2

Cooper, W. A., Lasher-Trapp, S. G., & Blyth, A. M. (2013). The influence of entrainment and mixing on the initial formation of rain in a warm cumulus cloud. *Journal of the Atmospheric Sciences*, *70*(6), 1727–1743. https://doi.org/10.1175/JAS-D-12-0128.1

Denby, L. (2020). Discovering the importance of mesoscale cloud organization through unsupervised classification. *Geophysical Research Letters*, *47*(1), 1–10. https://doi.org/10.1029/2019GL085190

Dipankar, A., Stevens, B., Heinze, R., Moseley, C., Zängl, G., Giorgetta, M., & Brdar, S. (2015). Large eddy simulation using the general circulation model ICON. *Journal of Advances in Modeling Earth Systems*, *7*(3), 963–986. https://doi.org/10.1002/2015MS000431

Feingold, G., McComiskey, A., Rosenfeld, D., & Sorooshian, A. (2013). On the relationship between cloud contact time and precipitation susceptibility to aerosol. *Journal of Geophysical Research: Atmospheres*, *118*(18), 10544–10554. https://doi.org/10.1002/jgrd.50819

Freud, E., & Rosenfeld, D. (2012). Linear relation between convective cloud drop number concentration and depth for rain initiation. *Journal of Geophysical Research*, *117*(D2), D02207. https://doi.org/10.1029/2011JD016457

George, G., Stevens, B., Bony, S., Vogel, R., & Naumann, A. K. (2023). Widespread shallow mesoscale circulations observed in the trades. *Nature Geoscience*, *16*, 584–589. https://doi.org/10.1038/s41561-023-01215-1

Hagen, M., Ewald, F., Groß, S., Oswald, L., Farrell, D. A., Forde, M., et al. (2021). Deployment of the C-band radar Poldirad on Barbados during EUREC⁴A. *Earth System Science Data*, *13*(12), 5899–5914. https://doi.org/10.5194/essd-13-5899-2021

Janssens, M., Vilà-Guerau de Arellano, J., Scheffer, M., Antonissen, C., Siebesma, A. P., & Glassmeier, F. (2021). Cloud patterns in the trades have four interpretable dimensions. *Geophysical Research Letters*, *48*(5), e2020GL091001. https://doi.org/10.1029/2020GL091001

Klocke, D., Brueck, M., Hohenegger, C., & Stevens, B. (2017). Rediscovery of the doldrums in storm-resolving simulations over the tropical Atlantic/704/106/704/106/35/704/106/35/823 perspective. *Nature Geoscience*, *10*(12), 891–896. https://doi.org/10.1038/s41561-017-0005-4

Langhans, W., Yeo, K., & Romps, D. M. (2015). Lagrangian investigation of the precipitation efficiency of convective clouds. *Journal of the Atmospheric Sciences*, *72*(3), 1045–1062. https://doi.org/10.1175/JAS-D-14-0159.1

Lau, K. M., & Wu, H. T. (2003). Warm rain processes over tropical oceans and climate implications. *Geophysical Research Letters*, *30*(24), 2–6. https://doi.org/10.1029/2003GL018567

Louf, V., Jakob, C., Protat, A., Bergemann, M., & Narsey, S. (2019). The relationship of cloud number and size with their large-scale environment in deep tropical convection. *Geophysical Research Letters*, *46*(15), 9203–9212. https://doi.org/10.1029/2019GL083964

Lutsko, N. J., & Cronin, T. W. (2018). Increase in precipitation efficiency with surface warming in radiative-convective equilibrium. *Journal of Advances in Modeling Earth Systems*, *10*(11), 2992–3010. https://doi.org/10.1029/2018MS001482

Mapes, B., & Neale, R. (2011). Parameterizing convective organization to escape the entrainment dilemma. *Journal of Advances in Modeling Earth Systems*, *3*(2). https://doi.org/10.1029/2011MS000042

Muller, C., & Takayabu, Y. (2020). Response of precipitation extremes to warming: What have we learned from theory and idealized cloud-resolving simulations, and what remains to be learned? *Environmental Research Letters*, *15*(3), 035001. https://doi.org/10.1088/1748-9326/ab7130

Narenpitak, P., Kazil, J., Yamaguchi, T., Quinn, P., & Feingold, G. (2021). From sugar to flowers: A transition of shallow cumulus organization during ATOMIC. *Journal of Advances in Modeling Earth Systems*, *13*(10), e2021MS002619. https://doi.org/10.1029/2021MS002619

Naumann, A. K., & Seifert, A. (2016). Recirculation and growth of raindrops in simulated shallow cumulus. *Journal of Advances in Modeling Earth Systems*, *8*(2), 520–537. https://doi.org/10.1002/2016MS000631

Nuijens, L., & Siebesma, A. P. (2019). Boundary layer clouds and convection over subtropical oceans in our current and in a warmer climate. *Current Climate Change Reports*, *5*(2), 80–94. https://doi.org/10.1007/s40641-019-00126-x

Nuijens, L., Stevens, B., & Siebesma, A. P. (2009). The environment of precipitating shallow cumulus convection. *Journal of the Atmospheric Sciences*, *66*(7), 1962–1979. https://doi.org/10.1175/2008JAS2841.1

Orlanski, I. (1975). A rational subdivision of scales for atmospheric processes. *Bulletin of the American Meteorological Society*, *56*(5), 527–530.

Radtke, J., Naumann, A. K., Hagen, M., & Ament, F. (2022). The relationship between precipitation and its spatial pattern in the trades observed during EUREC⁴A. *Quarterly Journal of the Royal Meteorological Society*, *148*(745), 1913–1928. https://doi.org/10.1002/qj.4284

Rauber, R. M., Stevens, B., Ochs, H. T., Knight, C., Albrecht, B. A., Blyth, A. M., et al. (2007). Over the ocean: The RICO campaign. *Bulletin of the American Meteorological Society*, *88*(12), 1912–1928. https://doi.org/10.1175/BAMS-88-12-1912

Rogers, R. R., & Yau, M. K. (1996). *A short course in cloud physics* (3rd ed, Vol. 113). Butterworth Heinemann.

Sarkar, M., Bailey, A., Blossey, P., de Szoeke, S. P., Noone, D., Quinones Melendez, E., et al. (2022). Sub-cloud rain evaporation in the North Atlantic ocean. *EGUsphere*, 1–37. https://doi.org/10.5194/egusphere-2022-1143

Schulz, H., Eastman, R., & Stevens, B. (2021). Characterization and evolution of organized shallow convection in the downstream North Atlantic trades. *Journal of Geophysical Research: Atmospheres*, *126*(17), e2021JD034575. https://doi.org/10.1029/2021JD034575

Schulz, H., & Stevens, B. (2023). Evaluating large-domain, hecto-meter, large-eddy simulations of trade-wind clouds using EUREC⁴A data. *Journal of Advances in Modeling Earth Systems*, *15*, e2023MS003648. https://doi.org/10.1029/2023MS003648

Seifert, A., & Beheng, K. D. (2001). A double-moment parameterization for simulating autoconversion, accretion and selfcollection. *Atmospheric Research*, *59*(60), 265–281. https://doi.org/10.1016/S0169-8095(01)00126-0

Seifert, A., & Beheng, K. D. (2006). A two-moment cloud microphysics parameterization for mixed-phase clouds. Part 1: Model description. *Meteorology and Atmospheric Physics*, *92*(1–2), 45–66. https://doi.org/10.1007/s00703-005-0112-4

Seifert, A., & Heus, T. (2013). Large-eddy simulation of organized precipitating trade wind cumulus clouds. *Atmospheric Chemistry and Physics*, *13*(11), 5631–5645. https://doi.org/10.5194/acp-13-5631-2013

Seifert, A., Heus, T., Pincus, R., & Stevens, B. (2015). Large-eddy simulation of the transient and near-equilibrium behavior of precipitating shallow convection. *Journal of Advances in Modeling Earth Systems*, *7*(4), 1918–1937. https://doi.org/10.1002/2015MS000489

Seifert, A., & Stevens, B. (2010). Microphysical scaling relations in a kinematic model of isolated shallow cumulus clouds. *Journal of the Atmospheric Sciences*, *67*(5), 1575–1590. https://doi.org/10.1175/2009JAS3319.1

Short, D. A., & Nakamura, K. (2000). TRMM radar observations of shallow precipitation over the tropical oceans. *Journal of Climate*, *13*(23), 4107–4124. https://doi.org/10.1175/1520-0442(2000)013⟨4107:TROOSP⟩2.0.CO;2

Siebesma, A. P. (1998). Shallow cumulus convection. In E. J. Plate, E. E. Fedorovich, D. X. Viegas, & J. C. Wyngaard (Eds.), *Buoyant convection in geophysical flows* (pp. 441–486). Springer Netherlands. https://doi.org/10.1007/978-94-011-5058-3_19

Snodgrass, E. R., Di Girolamo, L., & Rauber, R. M. (2009). Precipitation characteristics of trade wind clouds during RICO derived from Radar, Satellite, and aircraft measurements. *Journal of Applied Meteorology and Climatology*, *48*(3), 464–483. https://doi.org/10.1175/2008JAMC1946.1

Squires, P. (1958). The microstructure and colloidal stability of warm clouds. *Tellus*, *10*(2), 256–261. https://doi.org/10.1111/j.2153-3490.1958.tb02011.x

Stevens, B. (2005). Atmospheric moist convection. *Annual Review of Earth and Planetary Sciences*, *33*(1), 605–643. https://doi.org/10.1146/annurev.earth.33.092203.122658

Stevens, B., Bony, S., Brogniez, H., Hentgen, L., Hohenegger, C., Kiemle, C., et al. (2020). Sugar, gravel, fish and flowers: Mesoscale cloud patterns in the trade winds. *Quarterly Journal of the Royal Meteorological Society*, *146*(726), 141–152. https://doi.org/10.1002/qj.3662

Stevens, B., Bony, S., Farrell, D., Ament, F., Blyth, A., Fairall, C., et al. (2021). EUREC⁴A. *Earth System Science Data*, *13*(8), 4067–4119. https://doi.org/10.5194/essd-13-4067-2021

Stevens, B., & Feingold, G. (2009). Untangling aerosol effects on clouds and precipitation in a buffered system. *Nature*, *461*(7264), 607–613. https://doi.org/10.1038/nature08281

Sui, C.-H., Satoh, M., & Suzuki, K. (2020). Precipitation efficiency and its role in cloud-radiative feedbacks to climate variability. *Journal of the Meteorological Society of Japan Series II*, *98*(2), 261–282. https://doi.org/10.2151/jmsj.2020-024

Tompkins, A. M., & Semie, A. G. (2017). Organization of tropical convection in low vertical wind shears: Role of updraft entrainment. *Journal of Advances in Modeling Earth Systems*, *9*(2), 1046–1068. https://doi.org/10.1002/2016MS000802

Touzé-Peiffer, L., Vogel, R., & Rochetin, N. (2022). Cold pools observed during EUREC⁴A: Detection and characterization from atmospheric soundings. *Journal of Applied Meteorology and Climatology*, *61*(5), 593–610. https://doi.org/10.1175/JAMC-D-21-0048.1

van Zanten, M. C., Stevens, B., Nuijens, L., Siebesma, A. P., Ackerman, A. S., Burnet, F., et al. (2011). Controls on precipitation and cloudiness in simulations of trade-wind cumulus as observed during RICO. *Journal of Advances in Modeling Earth Systems*, *3*(2). https://doi.org/10.1029/2011MS000056

Vial, J., Dufresne, J. L., & Bony, S. (2013). On the interpretation of inter-model spread in CMIP5 climate sensitivity estimates. *Climate Dynamics*, *41*(11–12), 3339–3362. https://doi.org/10.1007/s00382-013-1725-9

Vogel, R., Konow, H., Schulz, H., & Zuidema, P. (2021). A climatology of trade-wind cumulus cold pools and their link to mesoscale cloud organization. *Atmospheric Chemistry and Physics*, *21*(21), 16609–16630. https://doi.org/10.5194/acp-21-16609-2021

Yamaguchi, T., Feingold, G., & Kazil, J. (2019). Aerosol-cloud interactions in trade wind cumulus clouds and the role of vertical wind shear. *Journal of Geophysical Research: Atmospheres*, *124*(22), 12244–12261. https://doi.org/10.1029/2019JD031073

Zängl, G., Reinert, D., Rípodas, P., & Baldauf, M. (2015). The ICON (ICOsahedral Non-hydrostatic) modelling framework of DWD and MPI-M: Description of the non-hydrostatic dynamical core. *Quarterly Journal of the Royal Meteorological Society*, *141*(687), 563–579. https://doi.org/10.1002/qj.2378